The International Journal of Advanced Manufacturing Technology (2024) 130:903–913
https://doi.org/10.1007/s00170-023-12747-6

ORIGINAL ARTICLE

Improving bonding strength by non-thermal atmospheric pressure plasma-assisted technology for A5052/PEEK direct joining

Kosuke Takenaka[1] · Akiya Jinda[1] · Soutaro Nakamoto[1] · Ryosuke Koyari[1] · Susumu Toko[1] · Giichiro Uchida[2] · Yuichi Setsuhara[1]

Received: 24 August 2023 / Accepted: 23 November 2023 / Published online: 6 December 2023

Abstract
The direct bonding of A5052 aluminum (Al) alloy to the engineering polymer poly(ether ether ketone) (PEEK) using an atmospheric pressure plasma-assisted process was demonstrated. The effect of plasma irradiation on the bonding surface of metal resin on the bonding strength following thermal press fitting method was investigated. Specimens bonded by plasma irradiation on the PEEK surface only showed a high tensile shear stress of 15.5 MPa. With increasing plasma irradiation time, the bond strength of the samples bonded to the PEEK surface by plasma irradiation increased. The increase in the bond strength between metals and polymers following direct bonding is caused by the addition of oxygen functional groups on the polymer. In contrast, specimens in which only the Al was exposed to the plasma showed a decrease in bond strength compared with unirradiated samples. This reduction in bond strength is attributed to the forming magnesium oxide, which forms in the early stages of participation due to plasma irradiation.

Keywords Dissimilar material joining · Atmospheric pressure plasma · Direct joint

1 Introduction

Multi-material hybrid structures exhibit various useful properties, including both low density and high performance. In particular, metal-polymer hybrids are expected to replace metals in industrial applications because they can reduce weight compared with pure metals and so lower costs, such as by providing improved fuel efficiency in the aerospace and automotive sectors [1–5]. Thermoplastics are also advantageous because they can be joined without the use of adhesives [6, 7] or items such as screws and rivets [8, 9]. To date, these materials have been joined via thermal press fitting using ultrasonic [10–12], induction [13], laser [14–17] or solid friction [18] heat sources. The metals-polymers direct bonding is known to result primarily from hydrogen bonds between oxides formed on metal surfaces and polar functional groups (amino groups, hydroxyl groups, carboxyl groups, etc.) present on polymers. Thus, the addition of functional groups to the surface of polymer using some surface treatment methods is required to obtain high strength, high quality direct metal-polymer bonding. At present, these surface treatment methods include chemical etching using acids and bases [19] and exposure to ultraviolet radiation [20], coronas [21] or plasmas [22]. Among these, plasma treatments are considered to be superior in that these techniques can modify only the polymer surface [22].

The present study performed surface treatments employing an atmospheric pressure plasma jet excited by radio frequency (RF) power. The oxygen radical density in such plasmas is two orders of magnitude higher than that in conventional high-voltage low-frequency atmospheric pressure plasma jets [23, 24]. On this basis, the process demonstrated herein was expected to efficiently add polar functional groups on polymer surfaces. In a prior work, stainless (SUS304) steel and polycarbonate (PC) were joined by joining technology by a combination

✉ Kosuke Takenaka
k_takenaka@jwri.osaka-u.ac.jp

[1] Joining and Welding Research Institute, Osaka University, 11-1 Mihogaoka, Ibaraki, Osaka 567-0047, Japan

[2] Faculty of Science and Technology, Meijo University, 1-501 Shiogamaguchi, Tempaku-ku, Nagoya 468-8502, Japan

of atmospheric pressure RF plasma jet and thermal press fitting [25].

In engineering plastics including PC and PEEK, it is difficult to modify the polymer surfaces using a low-frequency pulse plasma source because the irradiated surface is not heated to the temperature required for the surface reaction of radicals generated by low-frequency pulse plasma irradiation [25]. The atmospheric pressure RF-excited atmospheric plasma jet used in this study is more efficient than the common low-frequency high-voltage pulsed atmospheric plasma, since the plasma jet not only produces high-density plasmas but also promotes surface reactions by heating through plasma irradiation, thus allowing the surface treatment of the polymer and the metal without preheating the surface with other heating sources [25]. The results of this previous research demonstrated the feasibility of bonding metal-polymer dissimilar materials using this technology.

Modern automobile bodies often incorporate aluminum (Al) alloys or hybrids of Al alloys with other

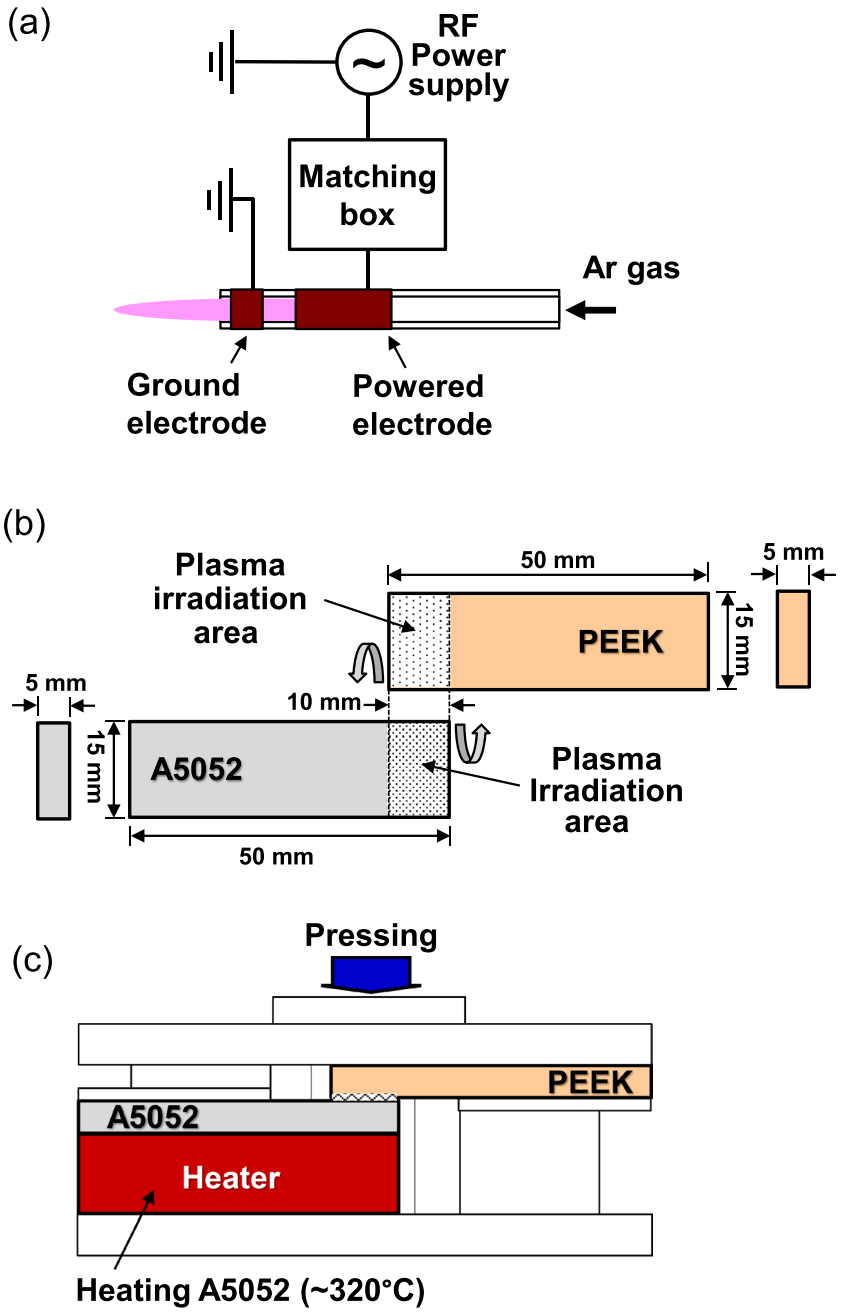

Fig. 1 Diagrams showing (**a**) the apparatus used to generate an atmospheric pressure RF plasma jet, (**b**) the dimensions of the specimen and (**c**) tensile-shear configuration for A5052 and PEEK direct joining with thermal press fitting via pre-plasma treatment

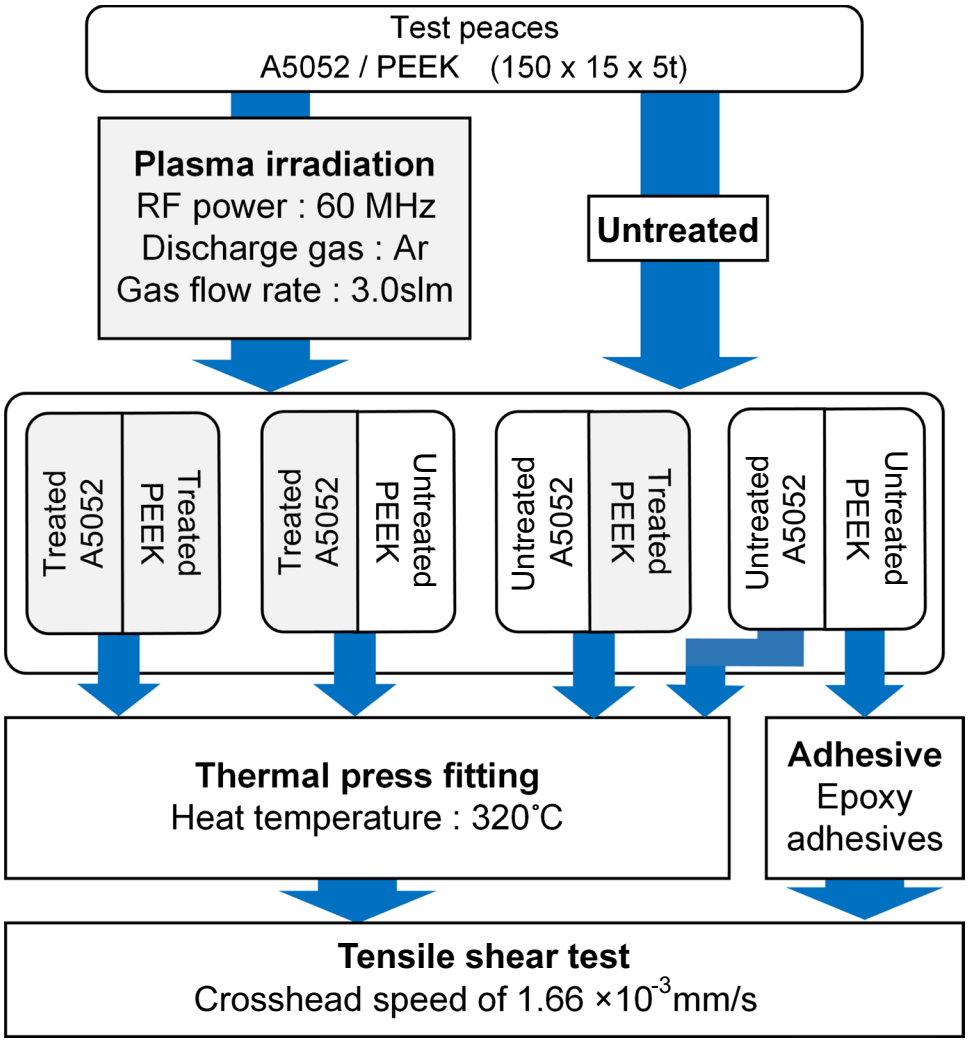

Fig. 2 Procedure for metal-polymer direct joining based on atmospheric pressure RF plasma jet irradiation

materials to achieve both weight reduction and rigidity [1, 26–29]. Thus, the development of technologies for the joining of Al alloys to materials such as engineering plastics is desirable. In the work reported herein, direct joining of an Al alloy (A5052) to the engineering plastic (poly ether ether ketone: PEEK) was performed using the plasma-assisted process and the influence of irradiating an atmospheric pressure plasma on the bonding strength of A5052-PEEK joints was investigated.

2 Experimental procedures

An atmospheric pressure RF plasma jet using Ar gas was employed for plasma-assisted direct joining. The plasma source consisted of a quartz tube wound with a wide (15 mm) metal strip serving as the electrode, to which high-frequency power was applied, and a narrow (5 mm) strip acting as a ground electrode (Fig. 1(a)). The narrow electrode (grounding electrode) was located at the quartz tube end along the path of gas flow, while the wide electrode to which RF power is applied was situated 5 mm from the top edge of the narrow electrode. A quartz tube (outer diameter: 6 mm and inner diameter: 4 mm) was used and high-frequency (60 MHz) sine wave power was applied to the power electrode. The pure Ar was feed to the plasma source at 3slm in gas flow rate [23, 24].

The test pieces used in this work comprised sheets of Al alloy (A5052) or PEEK (Mitsubishi chemical advanced materials, Ketron 1000), both having 500 mm × 15 mm × 5 mm in dimensions. Figure 1(b) and (c) shows the dimensions of the specimen and tensile-shear configuration for A5052 and PEEK direct joining with thermal press fitting via pre-plasma treatment. Figure 2 shows the procedure for metal-polymer direct joining based on atmospheric pressure RF plasma jet irradiation.

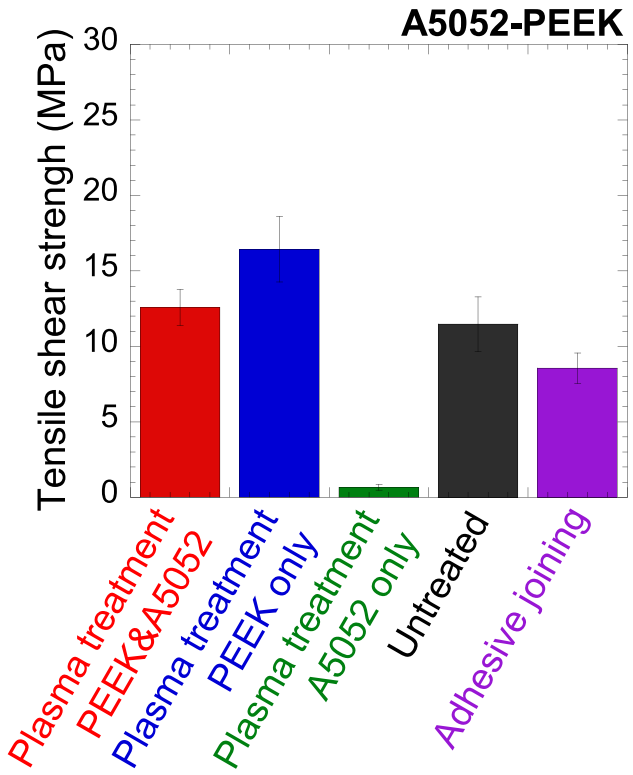

Fig. 3 Tensile shear strength for samples jointed by the thermal press fitting after plasma irradiation or the thermal press fitting with untreated A5052 and PEEK

In this process, the plasma jet was applied to the surfaces of one or both materials as a pre-treatment. After exposure to plasma, A5052 was heated by a heater until the temperature of A5052 reached 320°C, close to the melting point of PEEK, and then thermal press fitting was performed. The test pieces of metal and polymer were joined such that the two materials overlapped by 10 mm.

In order to evaluate bond strength, specimens were also bonded using an epoxy adhesive and the tensile shear stress for these samples was compared with that for specimens jointed using the thermal press fitting. Tensile tests were demonstrated employing a tensile tester (Autograph AGS-X, Shimadzu Corp.). In this measurement, a shear force acted on the bond interface at a crosshead speed of 1.66×10^{-3} mm/s and a tensile shear stress was evaluated by measuring the maximum load at failure of specimens bonded under various conditions the maximum load at failure for specimens bonded under various conditions.

To investigate the physical properties of surfaces after irradiation of plasma, the surface morphology of A5052 was assessed using scanning electron microscopy (SEM, Hitachi SU-70) together with energy dispersive X-ray spectroscopy (EDX, INCA PentaFETx3, Oxford Instruments) and atomic force microscopy (AFM, KEYENCE VN-8000). To evaluate the chemical properties of surfaces after plasma irradiation, the chemical bonding state of a surface of plasma-exposed polymer was analyzed using X ray photoelectron spectroscopy (XPS, AXIS165, Shimadzu).

3 Results and discussion

The plasma irradiation effect of the A5052 and PEEK surfaces on the bond was assessed by applying plasma treatments to only the A5052 or the PEEK or to both. Figure 3 summarizes the tensile shear strength for the various A5052-PEEK samples bonded using a combination of the thermal press fitting method and the plasma-assisted joining. The results of a sample of untreated A5052 and PEEK bonded by thermal press fitting and adhesive are also shown in Fig. 3 for comparison. The tensile shear strength of specimens of untreated A5052 and PEEK bonded by thermal press fitting and adhesive was 10.2 and 8.6 MPa. In bonding with epoxy adhesives, it is known that the bonding is achieved by hydrogen bonding or ionic bonding between functional groups such as OH and NH in the epoxy resin and oxygen functional groups present on the metal/polymer surface [30, 31]. Therefore, it is considered that adhesive and t thermal press fitting result in almost the same bond strength because adhesion and thermal bonding are similar bonding mechanisms. The average bond strength for the samples for which only the A5052 was exposed to the plasma was 0.6 MPa. In contrast, exposing only the PEEK to the plasma produced a significant increase in bond strength to 15.5 MPa, and the bond strength was greater than that for the unirradiated samples by a factor of 1.5. On the other hand, the bond strength of the sample plasma-treated with both A5052 and PEEK was 12.1 MPa, which was slightly lower than that of the sample irradiated only with PEEK. Figure 4 presents photographic images of the fracture surfaces of specimens bonded with and without plasma irradiation after tensile testing. The plasma irradiation on the A5052 side caused greater delamination, and cohesive breakdown was observed only in a small area. On the other hand, the sample without plasma irradiation on the A5052 side showed cohesive breakdown of PEEK in a larger area than in the sample with plasma

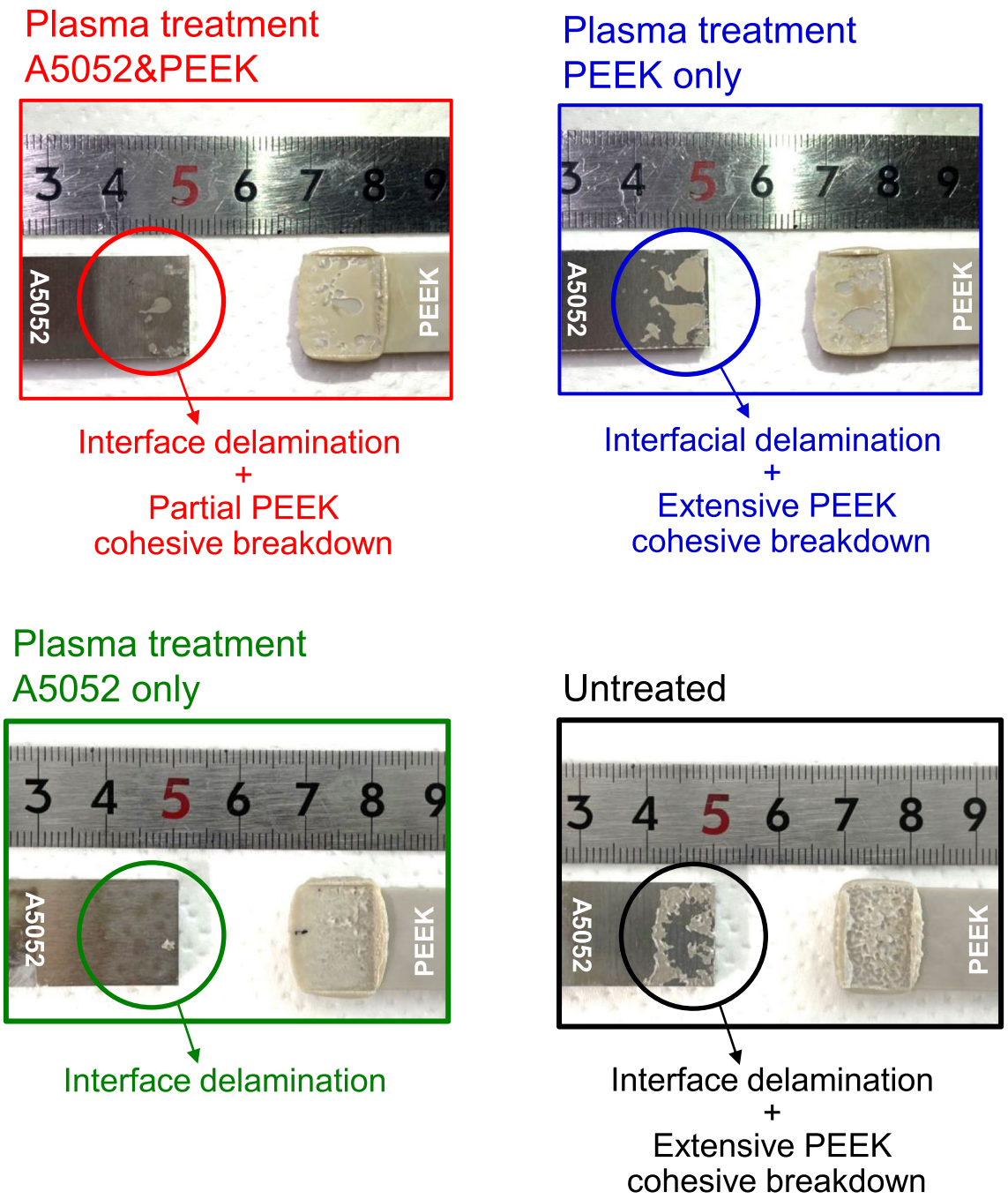

Fig. 4 Photographic images of fracture surfaces after tensile testing of specimens bonded with and without plasma irradiation

irradiation on A5052 side, although delamination of the interface was also pronounced. These results indicate that the plasma treatment of PEEK is effective in improving bond strength in the direct bonding of A5052-PEEK. In contrast, specimens in which the metal had been irradiated exhibited decreased bond strength.

To investigate the cause of the decrease in bond strength due to plasma irradiation of A5052, the physical and chemical analysis of the A5052 surface before and after plasma irradiation was performed. The physical and chemical states of material surfaces are known to play important roles in the direct joining of dissimilar materials. The

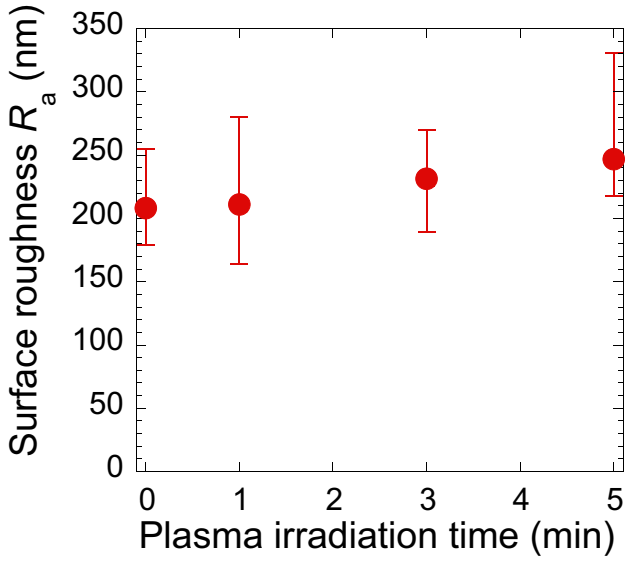

Fig. 5 Variation in surface roughness, R_a, for A5052 with plasma irradiation time

surface morphology of A5052 surfaces before and after irradiation of the plasma was observed using AFM. Figure 5 plots the surface roughness, R_a, as estimated from AFM images as a function of exposure time. With increasing plasma irradiation time, the R_a of the A5052 surface increased slightly, from 208 nm at 0 min (that is, the pristine surface) to 247 nm after 5 min. Considering the physical aspects of joining dissimilar materials, it is generally known that an increase in surface roughness R_a increases the bond strength due to the mechanical interlocking (anchor effect). However, when A5052 is irradiated with plasma, bonding strength is dramatically improved with plasma irradiation compared to PEEK without plasma irradiation. On the other hand, there is only a slight increase in surface roughness due to plasma irradiation. Therefore, these data suggest that the influence of physical effects including anchor effect on the difference in bond strength with and without plasma irradiation of PEEK is small. In a previous study, it was confirmed that plasma irradiation adds oxygen functional groups (C=O and O-C=O) to the PEEK surface, and that the oxygen functional groups increase with increasing plasma irradiation time. [32] In this experiment, there was no significant increase in the surface roughness of A5052 due to plasma irradiation, and the bond strength increased only due to plasma irradiation on the PEEK side. These results indicate that the addition of functional group on PEEK surface, not the anchoring effect on the A5052 side, contributed to the increase in bond strength. These data therefore confirm that the increased bond strength of the samples after plasma exposure was primarily a result of chemical effects rather than physical effects.

Variation in the chemical composition of the surface of A5052 after irradiation of the plasma was also investigated by SEM-EDX. Figure 6 provides SEM images and SEM-EDX elemental maps of Al (blue), Mg (purple), O (red), Cr (yellow) and Fe (green) acquired from the surface of A5052 before and after 5 min of plasma exposure. These images indicate that minimal physical change was induced by irradiation. However, the O maps show some slight oxidation while the Mg maps indicate a significant increase in the amount of Mg across the entire metal surface after plasma treatment. Figure 7 summarizes the Mg/Al and O/Al ratios estimated from SEM-EDX elemental maps as functions of the plasma irradiation time. These results demonstrate that the plasma treatment increased the concentrations of both O and Mg on the A5052 surface. The increase in the relative atomic concentration of O is due to oxidation on A5052 by reactive oxygen species generated by the plasma jet.

The chemical bonding state of the surface of A5052 before and after irradiation of the plasma was examined using XPS. Figure 8 presents Al 2p, Mg 2p and O 1s XPS spectra of treated and untreated specimens. The Al 2p spectra could be deconvoluted into peaks related to Al (metal) at 71.8 eV and Al_2O_3 at 74.5 eV [33]. The Mg 2p spectra were deconvoluted into peaks related to Mg (metal), magnesium oxide (MgO) and hydroxides/oxides at 49.6, 50.8 and 51.6 eV, respectively [34, 35]. The O 1s spectra were deconvoluted into peaks associated with oxides and hydroxides at 531.3 and 532.8 eV [36]. The Al 2p spectrum of the pristine A5052 exhibited peaks related to AlO_x and metallic Al while the Mg 2p spectrum showed only a low-intensity peak. The O 1s spectrum contained peaks attributed to a natural oxide film. Following plasma irradiation, the data indicated an increase in the amount of MgO on the A5052 surface. These results demonstrate that the alloy was initially covered with an AlO_x coating without Mg but that a MgO layer was formed as Mg diffused to the surface as a consequence of the heat input from the plasma [37–39]. The presence of MgO as the major phase can be explained by the rapid growth rate of MgO. It is possible that in the early stages of oxidation, Mg has diffused rapidly through local paths of easy diffusion in the alloy surface forming MgO. Surface inhomogenities (rolling defects), dislocations, and grain boundaries could serve as short-circuit paths for diffusion of Mg. Usually, MgO does not form a continuous layer [40, 41].

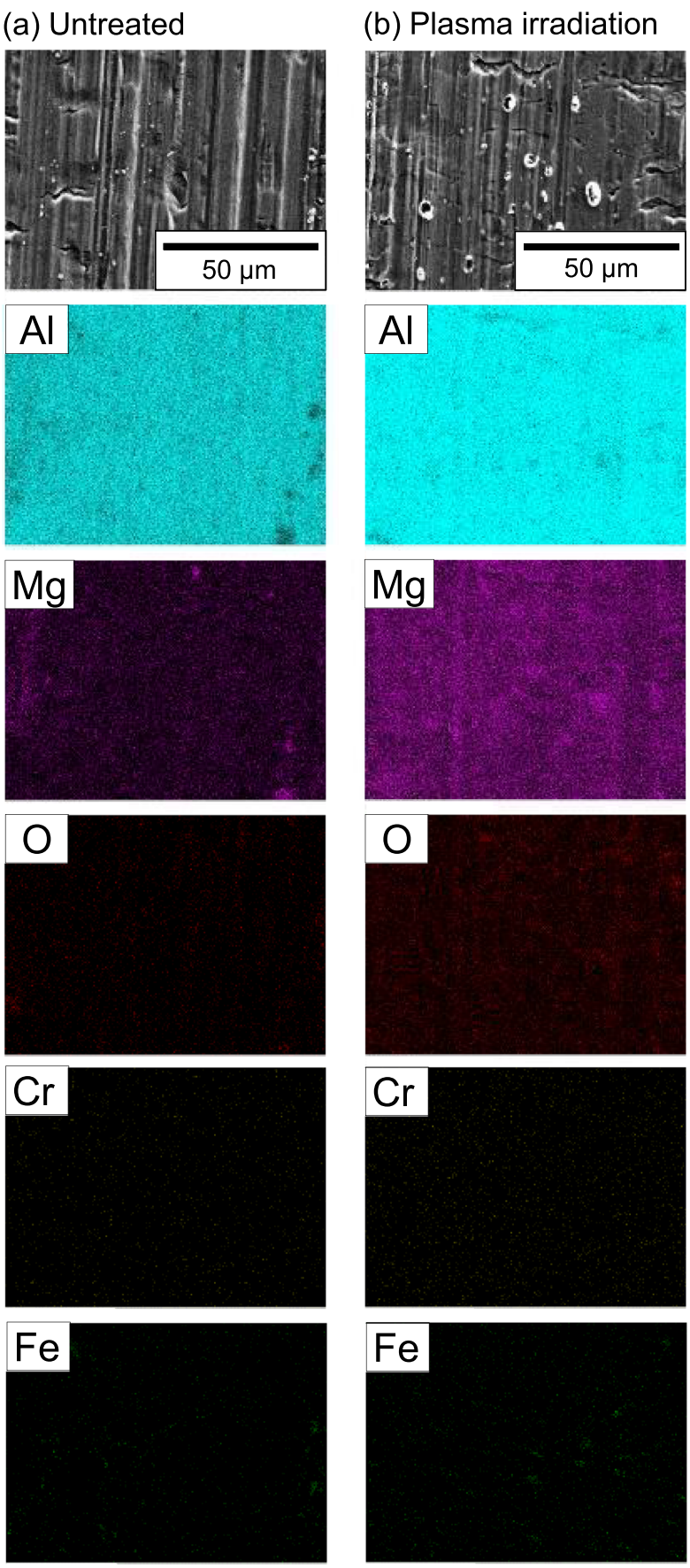

Fig. 6 SEM images and SEM-EDX elemental maps of Al (blue), Mg (purple), O (red), Cr (yellow) and Fe (green) on the surface of (**a**) untreated A5052 and (**b**) A5052 exposed to plasma for 5 min

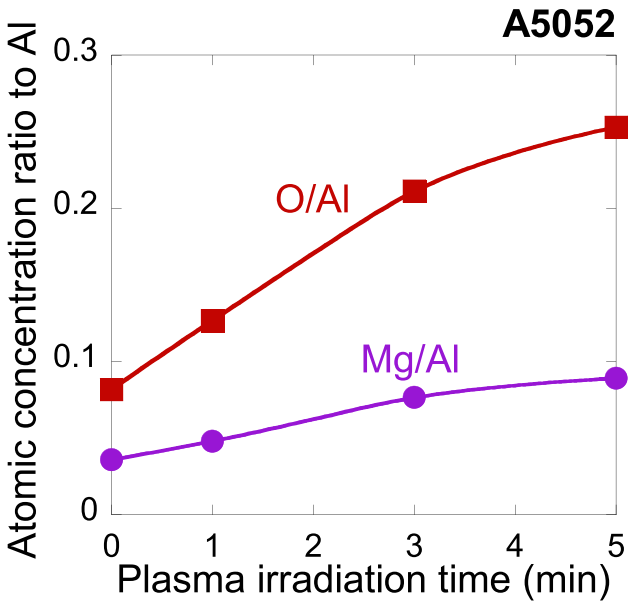

Fig. 7 Variation of the ratios of O and Mg to Al on an A5052 surface (as estimated from SEM-EDX elemental maps) with plasma irradiation time

This MgO is thought to have decreased the bond strength. Other work has shown that the adhesion and ageing of paints [42, 43] and adhesives [44] on metals having a MgO surface layer are frequently poor because of the friability and susceptibility to hydrolysis of the oxide [39]. Typically, MgO formed on Al-Mg alloys such as A5052 via diffusion of Mg will show low cohesive strength and is easily chemically fed to form oxides and thus to generate weakly bonded layers [45]. The present results suggest that the migration of Mg to the surface as a consequence of heating by the plasma with subsequent oxidation by radicals induced the formation of MgO. This, in turn, lowered the bond strength between the A5052 and PEEK.

The effect of exposing the PEEK side of A5052-PEEK specimens to the plasma was also investigated. Figure 9 plots the tensile shear strength of A5052-PEEK joints as a function of the time span over which the PEEK was treated with the plasma, with no treatment applied to the A5052. With increasing irradiation time, the bond strength evidently underwent a moderate increase from 10.2 MPa at 0 min to 15.5 MPa after 5 min and then was almost constant.

In a previous study, the effect of plasma irradiation on the chemical state of PEEK surfaces was assessed using XPS [32]. These prior XPS analyses indicated the O-C=O bond formation due to irradiation of the plasma, as well as C-O and C=O bonds that were originally present in the PEEK. The amount of each of these groups on the PEEK surface was found to increase as the plasma irradiation time was increased. It has been determined that O=C-O groups on the polymer increase the bond strength between metals and polymers following direct bonding [46–48]. Hence, these results suggest that oxidation of the PEEK by radicals in the atmospheric pressure RF plasma jet generated oxygen-containing surface functional groups that increased the bond strength.

4 Conclusions

Direct bonding of an Al alloy to PEEK via non-thermal atmospheric pressure plasma-assisted joining technology has been demonstrated. The effect of plasma irradiation on the bond strength following thermal press fitting was investigated. The tensile shear strength of A5052-PEEK joined by thermal press fitting with plasma-assisted joining was established by comparison with specimens made using conventional thermal press fitting and adhesive bonding. The tensile shear stress for samples bonded after irradiation of the plasma of only the PEEK was as high as 15.5 MPa, 50% higher than that of the unirradiated sample. This improved bond strength can be attributed to the addition of oxygen-based functional groups on the surface of PEEK by radicals generated by plasma jet. In contrast, plasma treatment of the A5052 side led to a decrease in bond strength as a consequence of the generation of MgO, which formed on Al-Mg alloys such as A5052 via diffusion of Mg that will show low cohesive strength and is easily chemically fed to form oxides and thus to generate weakly bonded layers. This reduction in bond strength is attributed to the forming magnesium oxide, which forms in the early stages of participation due to plasma irradiation. The effect of exposing the PEEK side of A5052-PEEK specimens to the plasma was also investigated. With increasing irradiation time, the bond strength evidently underwent a moderate increase from 10.2 MPa at 0 min to 15.5 MPa after 5 min and then was almost constant. These results suggest that oxidation of the PEEK by radicals in the atmospheric pressure RF plasma jet generated oxygen-containing surface functional groups that increased the bond strength.

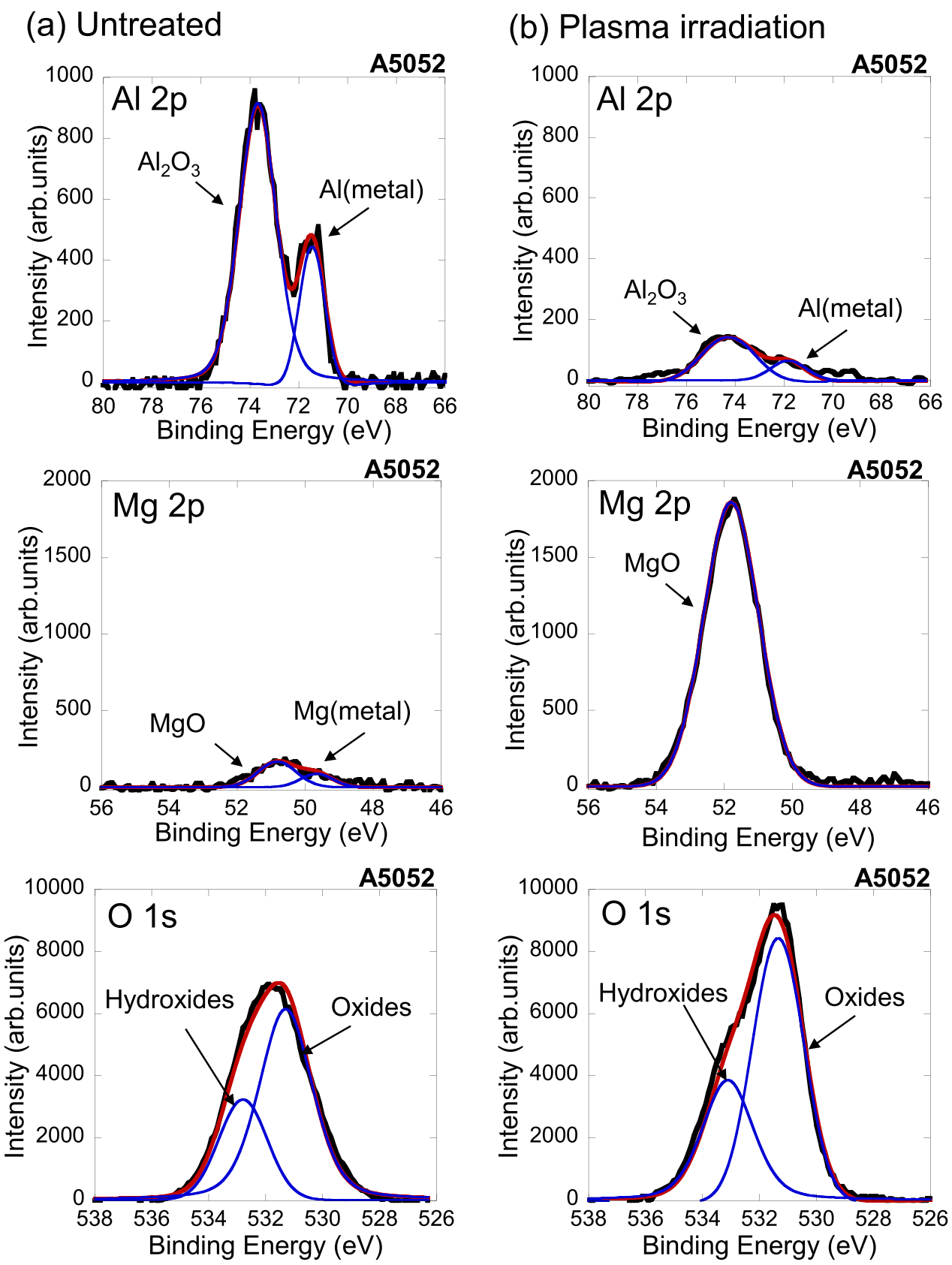

Fig. 8 Al 2p, Mg 2p and O 1s XPS spectra of an A5052 surface (**a**) without and (**b**) with plasma irradiation

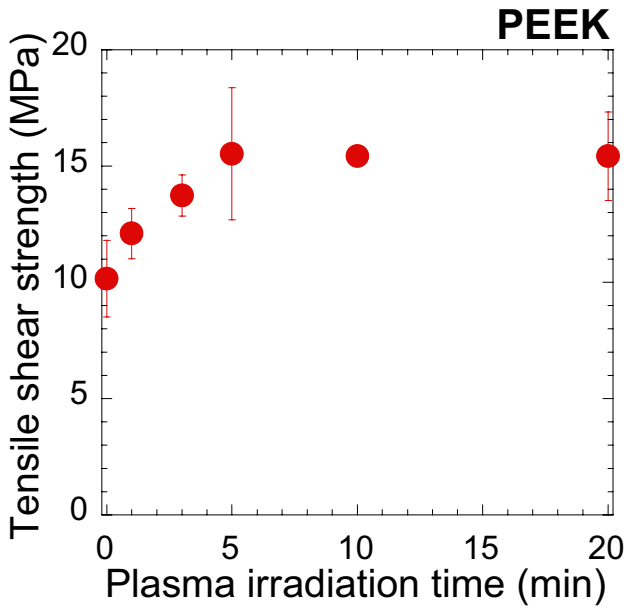

Fig. 9 Variation of the tensile shear strength of A5052-PEEK bonded samples following plasma treatment only of the PEEK side with plasma irradiation time

Author contributions Kosuke Takenaka contributed to all parts of this work: Conceptualization, Investigation, and Writing the manuscript. Akiya Jinda, Sotaro Nakamoto, Ryosuke Koyari and Susumu Toko contributed to collecting and analyzing the data of surface measurement and the joining experiments. Giichiro Uchida contributed to assistance of conceptualization, analyzing the data of investigation. Yuichi Setsuhara contributed to conceptualization, supervision, and project administration. All authors read and approved the final manuscript.

Funding Open access funding provided by Osaka University.

Declarations

Consent for publication The authors give the publisher the consent to publish the work.

Competing interests The authors declare no competing interests.

References

1. Lambiase F, Scipioni SI, Lee CJ et al (2021) A state-of-the-art review on advanced joining processes for metal-composite and metal-polymer hybrid structures. Materials 14. https://doi.org/10.3390/MA14081890
2. Mondal S (2021) Aluminum or its alloy matrix hybrid nanocomposites. Met Mater Int 27:2188–2204
3. Li SS, Yue X, Li QY, Peng HL, Dong BX, Liu TS, Yang HY, Fan J, Shu SL, Qiu F, Jiang QC (2023) Development and applications of aluminum alloys for aerospace industry. J Mater Res Technol 27:944–983. https://doi.org/10.1016/j.jmrt.2023.09.274
4. Han S, Guang X, Li Z, Li Y (2022) Joining processes of CFRP-Al sheets in automobile lightweighting technologies: a review. Polym Compos 43:8622–8633. https://doi.org/10.1002/pc.27088
5. Chandel R, Sharma N, Bansal SA (2021) A review on recent developments of aluminum-based hybrid composites for automotive applications. Emergent Mater 4:1243–1257. https://doi.org/10.1007/s42247-021-00186-6
6. Tong L (1998) Failure of adhesive-bonded composite single lap joints with embedded cracks. AIAA J 36:448–456. https://doi.org/10.2514/2.385
7. Cheuk PT, Tong L (2002) Failure of adhesive bonded composite lap shear joints with embedded precrack. Compos Sci Technol 62:1079–1095. https://doi.org/10.1016/S0266-3538(02)00054-4
8. Marannano G, Zuccarello B (2015) Numerical experimental analysis of hybrid double lap aluminum-CFRP joints. Compos B Eng 71:28–39. https://doi.org/10.1016/J.COMPOSITESB.2014.11.025
9. Amancio-Filho ST, Dos Santos JF (2009) Joining of polymers and polymer-metal hybrid structures: recent developments and trends. Polym Eng Sci 49:1461–1476. https://doi.org/10.1002/PEN.21424
10. Balle F, Wagner G, Eifler D (2007) Ultrasonic spot welding of aluminum sheet/ carbon fiber reinforced polymer - Joints. Materwiss Werksttech 38:934–938. https://doi.org/10.1002/MAWE.200700212
11. Balle F, Wagner G, Eifler D (2009) Ultrasonic metal welding of aluminium sheets to carbon fibre reinforced thermoplastic composites. Adv Eng Mater 11:35–39. https://doi.org/10.1002/ADEM.200800271
12. Balle F, Eifler D (2012) Statistical test planning for ultrasonic welding of dissimilar materials using the example of aluminum-carbon fiber reinforced polymers (CFRP) joints. Materwiss Werksttech 43:286–292. https://doi.org/10.1002/MAWE.201200943
13. Mitschang P, Velthuis R, Didi M (2013) Induction spot welding of metal/CFRPC hybrid joints. Adv Eng Mater 15:804–813. https://doi.org/10.1002/ADEM.201200273
14. Katayama S, Kawahito Y (2008) Laser direct joining of metal and plastic. Scr Mater 59:1247–1250. https://doi.org/10.1016/J.SCRIPTAMAT.2008.08.026
15. Lamberti C, Solchenbach T, Plapper P, Possart W (2014) Laser assisted joining of hybrid polyamide-aluminum structures. Phys Procedia 56:845–853. https://doi.org/10.1016/J.PHPRO.2014.08.103
16. Jung KW, Kawahito Y, Takahashi M, Katayama S (2013) Laser direct joining of carbon fiber reinforced plastic to zinc-coated steel. Mater Des 47:179–188. https://doi.org/10.1016/J.MATDES.2012.12.015
17. Davies RJ, Kinloch AJ (1989) The surface characterisation and adhesive bonding of aluminium. Adhesion 13:8–22. https://doi.org/10.1007/978-94-010-9082-7_2
18. Liu FC, Liao J, Nakata K (2014) Joining of metal to plastic using friction lap welding. Mater Des 54:236–244. https://doi.org/10.1016/J.MATDES.2013.08.056

19. Ha SW, Hauert R, Ernst KH, Wintermantel E (1997) Surface analysis of chemically-etched and plasma-treated polyetheretherketone (PEEK) for biomedical applications. Surf Coat Technol 96:293–299. https://doi.org/10.1016/S0257-8972(97)00179-5
20. Shi H, Sinke J, Benedictus R (2017) Surface modification of PEEK by UV irradiation for direct co-curing with carbon fibre reinforced epoxy prepregs. Int J Adhes Adhes 73:51–57. https://doi.org/10.1016/J.IJADHADH.2016.07.017
21. Comyn J, Mascia L, Xiao G, Parker BM (1996) Corona-discharge treatment of polyetheretherketone (PEEK) for adhesive bonding. Int J Adhes Adhes 16:301–304. https://doi.org/10.1016/S0143-7496(96)00010-3
22. Endo T, Reddy L, Nishikawa H et al (2017) Composite engineering - direct bonding of plastic PET films by plasma irradiation. Procedia Eng 171:88–103. https://doi.org/10.1016/J.PROENG.2017.01.315
23. Uchida G, Kawabata K, Ito T et al (2017) Development of a non-equilibrium 60 MHz plasma jet with a long discharge plume. J Appl Phys 122. https://doi.org/10.1063/1.4993715
24. Uchida G, Takenaka K, Takeda K et al (2018) Selective production of reactive oxygen and nitrogen species in the plasma-treated water by using a nonthermal high-frequency plasma jet. Jpn J Appl Phys 57. https://doi.org/10.7567/JJAP.57.0102B4
25. Takenaka K, Machida R, Bono T et al (2022) Development of a non-thermal atmospheric pressure plasma-assisted technology for the direct joining of metals with dissimilar materials. J Manuf Process 75:664–669. https://doi.org/10.1016/j.jmapro.2022.01.041
26. Martinsen K, Hu SJ, Carlson BE (2015) Joining of dissimilar materials. CIRP annals 64:679–699. https://doi.org/10.1016/J.CIRP.2015.05.006
27. Zhou Z, Gao X, Zhang Y (2022) Research progress on characterization and regulation of forming quality in laser joining of metal and polymer, and development trends of lightweight automotive applications. Metals 12:1666. https://doi.org/10.3390/MET12101666
28. Feistauer EE, dos Santos JF, Amancio-Filho ST (2019) A review on direct assembly of through-the-thickness reinforced metal–polymer composite hybrid structures. Polym Eng Sci 59:661–674. https://doi.org/10.1002/PEN.25022
29. Vasconcelos RL, Oliveira GHM, Amancio-Filho ST, Canto LB (2023) Injection overmolding of polymer-metal hybrid structures: a review. Polym Eng Sci 63:691–722. https://doi.org/10.1002/PEN.26244
30. Nakamae K, Nishino T, Airu X, Asaoka S (1995) Localization of the curing agent at an epoxy resin/oxidized aluminium interface. Int J Adhes Adhes 15:15–20. https://doi.org/10.1016/0143-7496(95)93638-2
31. Glazer J (1954) Monolayer studies of some ethoxylin resin adhesives and related compounds. J Polym Sci 13:355–369. https://doi.org/10.1002/pol.1954.120137004
32. Takenaka K, Jinda A, Nakamoto S, Toko S, Uchida G, Setsuhara Y (2023) Direct bonding of stainless steel and PEEK using non-thermal atmospheric pressure plasma-assisted joining technology. J Manuf Process 105:276–281. https://doi.org/10.1016/j.jmapro.2023.09.049
33. Strohmeier BR (1990) An ESCA method for determining the oxide thickness on aluminum alloys. Surface and Interface Analysis 15:51–56. https://doi.org/10.1002/SIA.740150109
34. Liu M, Zanna S, Ardelean H et al (2009) A preliminary quantitative XPS study of the surface films formed on pure magnesium and on magnesium-aluminium intermetallics by exposure to high-purity water. Materials Science Forum 618–619:255–262. https://doi.org/10.4028/WWW.SCIENTIFIC.NET/MSF.618-619.255
35. Chen C, Splinter SJ, Do T, McIntyre NS (1997) Measurement of oxide film growth on Mg and Al surfaces over extended periods using XPS. Surf Sci 382:L652–L657. https://doi.org/10.1016/S0039-6028(97)00054-X
36. Wang X, Lin JP, Min JY, Wang PC, Sun CC (2018) Effect of atmospheric pressure plasma treatment on strength of adhesive-bonded aluminum AA5052. J Adhesion 94:701–722. https://doi.org/10.1080/00218464.2017.1393747
37. Ritchie IM, Sanders JV, Weickhardt PL (1971) Oxidation of a dilute aluminum magnesium alloy. Oxidation of Metals 3:91–101. https://doi.org/10.1007/BF00604741/METRICS
38. Goldstein B, Dresner J (1978) Growth of MgO films with high secondary electron emission on Al-Mg alloys. Surf Sci 71:15–26. https://doi.org/10.1016/0039-6028(78)90310-2
39. Lea C, Ball J (1984) The oxidation of rolled and heat treated Al-Mg alloys. Applications of Surface Science 17:344–362. https://doi.org/10.1016/0378-5963(84)90023-0
40. Zayan MH, Jamjoom OM, Razik NA (1990) High-temperature oxidation of Al-Mg alloys. Oxid Met 34:323–333. https://doi.org/10.1007/BF00665021
41. Haginoya I, Fukusako T (1983) Oxidation of molten Al-Mg alloys. T Jpn I Met 24:613–619. https://doi.org/10.2320/matertrans1960.24.613
42. Guminski RD, Meredith FMP (1961) Lacquer coating of aluminium/magnesium alloys. J Oil Colour Chem Assoc 44:93
43. Kozma L, Olefjord I (2013) Basic processes of surface preparation and bond formation of adhesively joined aluminium. Mater Sci Tech-lond 3:860–874. https://doi.org/10.1179/MST.1987.3.10.860
44. Sun TS, Chen JM, Venables JD, Hopping R (1978) Effects of chemical and thermal treatments on the composition of 2024 aluminum adherend surfaces. Applications of Surface Science 1:202–214. https://doi.org/10.1016/0378-5963(78)90015-6
45. Field DJ, Scamans GM, Butler EP (1987) High temperature oxidation of Al-4. 2 Wt Pct Mg ALLOY. Metall Trans A 18A:463–472. https://doi.org/10.1007/BF02648807
46. Ochoa-Putman C, Vaidya UK (2011) Mechanisms of interfacial adhesion in metal–polymer composites – effect of chemical treatment. Compos Part A Appl Sci Manuf 42:906–915. https://doi.org/10.1016/J.COMPOSITESA.2011.03.019
47. Comyn J, Mascia L, Xiao G, Parker BM (1996) Plasma-treatment of polyether ether ketone (PEEK) for adhesive bonding. Int J Adhes Adhes 16:97–104. https://doi.org/10.1016/0143-7496(96)89798-3
48. Laurens P, Sadras B, Decobert F et al (1998) Enhancement of the adhesive bonding properties of PEEK by excimer laser treatment. Int J Adhes Adhes 18:19–27. https://doi.org/10.1016/S0143-7496(97)00063-8